A Waveguide-Based Aperture-Coupled Patch Amplifier Array—Full-Wave System Analysis and Experimental Validation

Alexander B. Yakovlev, *Member, IEEE*, Sean Ortiz, *Student Member, IEEE*, Mete Ozkar, *Student Member, IEEE*, Amir Mortazawi, *Member, IEEE*, and Michael B. Steer, *Fellow, IEEE*

***Abstract*—In this paper, the full-wave analysis and experimental verification of a waveguide-based aperture-coupled patch amplifier array are presented. The spatial power-combining amplifier array is modeled by the decomposition of the entire system into several electromagnetically coupled modules. This includes a method of moments integral equation formulation of the generalized scattering matrix (GSM) for an N-port waveguide-based patch-to-slot transition; a mode-matching analysis of the GSM for the receiving and transmitting rectangular waveguide tapers; and a finite-element analysis of the waveguide-to-microstrip line junctions. An overall response of the system is obtained by cascading GSMs of electromagnetic structures and the S-parameters of amplifier networks. Numerical and experimental results are presented for the single unit cell and 2×3 amplifier array operating at X-band. The results are shown for the rectangular aperture-coupled patch array, although the analysis is applicable to structures with arbitrarily shaped planar electric and magnetic surfaces.**

***Index Terms*—Amplifier network, dyadic Green's functions, generalized scattering matrix (GSM), integral equations, method of moments (MoM), patch, slot arrays, spatial power combining, waveguide transition.**

I. Introduction

THE DEMAND for high-power and efficient solid-state millimeter-wave amplifiers has initiated extensive theoretical and experimental research in the area of spatial and quasi-optical power combining arrays. Free-space power-combining systems were first developed nearly a decade ago, beginning with a grid amplifier [1]. This and other amplifiers to follow [2]–[5] were developed with the intent of exciting the array either by Gaussian beams or by locating the array in the far field of a feeding antenna, thereby minimizing the interaction between the antenna and the amplifier array. In contrast to free-space power-combining systems, waveguide-based quasi-optical amplifiers, developed in the past few years [6]–[14], are characterized by the placement of the amplifier array inside an oversized waveguide or in close proximity to a hard-horn antenna. The waveguide-based systems are more compact when compared to the free-space fed arrays, and can, therefore, be analyzed more efficiently.

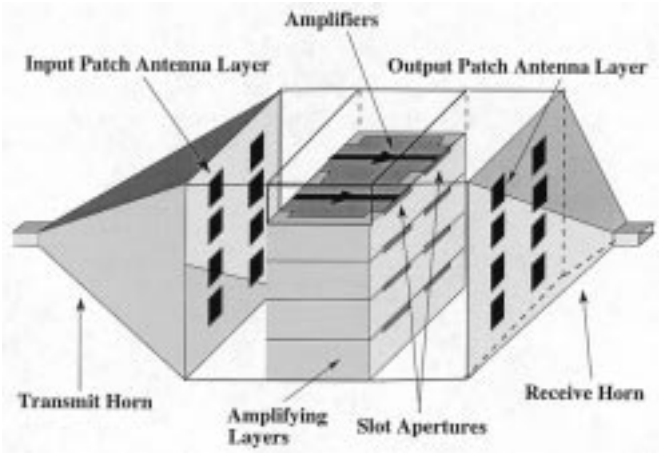

Fig. 1. A waveguide-based aperture-coupled patch amplifier array.

There is a great need for the electromagnetic modeling of spatial power-combining systems in order to increase the general understanding of the system behavior and to aid in the design process. To avoid the complexities of using only one electromagnetic modeling technique, the spatial power-combining amplifier array is decomposed into several modules. Each module is simulated using the most appropriate (efficient) and convenient numerical technique. An overall response of the system is then obtained by cascading the responses of the individual modules.

Fig. 1 represents the spatial power-combining system to be analyzed here. Recently, the amplifier array has been designed, fabricated, and tested using a hard-horn excitation that maintains a reasonably flat amplitude and phase variation across its aperture [15]. The incident signal from the transmit horn on the left of the figure couples to an array of aperture-coupled patch antennas. Each antenna is coupled to a dielectric-filled waveguide through the antenna aperture. The signal is then coupled from the waveguide to a microstrip circuit, containing matching networks and amplifiers. After amplification, the signal is coupled back to the dielectric-filled waveguide, reradiated through

Manuscript received February 24, 2000; revised August 25, 2000. This work was supported by the Army Research Office under the Spatial and Quasi-Optical Power Combining MURI Grant DAAG-55-97-0132. The work of S. Ortiz was also supported by an NSF Graduate Fellowship.

A. B. Yakovlev was with the Department of Electrical and Computer Engineering, North Carolina State University, Raleigh, NC 27695-7914 USA. He is now with the Department of Electrical Engineering, The University of Mississippi, University, MS 38677 USA (e-mail: yakovlev@ieee.org).

S. Ortiz, M. Ozkar, A. Mortazawi, and M. B. Steer are with the Department of Electrical and Computer Engineering, North Carolina State University, Raleigh, NC 27695-7914 USA.

Publisher Item Identifier S 0018-9480(00)10748-3.

0018–9480/00$10.00 © 2000 IEEE

an aperture-coupled patch antenna, and then collected by the receive horn.

This particular system has the benefit of isolating the microstrip circuitry, which may include amplifiers, matching networks, and biasing networks, from the radiating elements through the use of a unique antenna-feed first developed in [15]. In addition, the feed isolates the radiating element from the microstrip circuit by way of the dielectric-filled waveguide. This isolation is beneficial for both circuit design and simulation by separating the amplifier circuit from the antenna array.

In this paper, the complete model of the power-combining system is based upon cascading characterizations of individual components of the system. A full-wave integral equation formulation is proposed for the electromagnetic modeling of a waveguide-to-aperture-coupled patch array, resulting in the generalized scattering matrix (GSM) of the N-port spatial power divider/combiner. The coupled set of electric- and magnetic-field integral equations (with dyadic Green's functions obtained for semiinfinite layered waveguides) is discretized via method of moments (MoM) for the induced electric and magnetic surface current density. This provides an accurate model of the patch-to-slot coupling at each port for all propagating and evanescent TE and TM modes. Note that due to the complexity of the problem, general-purpose commercial electromagnetic packages based on volumetric gridding, such as the finite-element method (FEM) and the finite-difference time-domain method (FDTD), are unable to model the fields of large waveguide-based arrays as encountered with spatial power combiners. The work presented in this paper is a generalization of results obtained in [16] and [17] for the GSM of interactive arbitrarily shaped strip and slot discontinuities in a two-port waveguide transition. The GSM for a rectangular waveguide taper is obtained using a mode-matching technique, where a linear taper is approximated by double-plane stepped junctions similar to [18]. A waveguide-to-microstrip line transition was modeled using a three-dimensional (3-D) commercial FEM program [19]. All modules within the power-combining system, including the amplifier networks, are then cascaded to obtain the overall response (return loss and gain). The structure was simulated and tested for a single unit cell and 2 × 3 element amplifier array.

II. Full-Wave System Modeling

A. Introduction

The electromagnetic model of the spatial power-combining amplifier presented here (Fig. 1) is based on the decomposition of the system into modules, including rectangular waveguide tapers (feeding and collecting), N-port aperture-coupled patch array waveguide transitions (divider and combiner), waveguide-to-microstrip line junctions, and amplifier circuits. Each of these modules must be rigorously analyzed in order to accurately obtain the response of the system.

We first consider the N-port waveguide-based aperture-coupled patch array transition shown in Fig. 2. Rectangular patch antennas S_m^i and slot apertures S_s^j in a ground plane S_g are located on the opposite interfaces of the dielectric layer with permittivity ϵ_2. Note that each of the slot-coupled waveguides (regions V_s^j) is filled with the same dielectric material (ϵ_3). The incident electric and magnetic fields in the large waveguide (region V_1) are generated by an impressed electric current source $\overline{\mathbf{J}}_{\mathrm{imp}}$ ($\nabla \times \overline{\mathbf{J}}_{\mathrm{imp}}$ for the magnetic field). It should be noted that a similar treatment has been applied to each of the waveguides V_s^j in the multiport transition. The construction of the MoM matrix does not depend on the excitation, since the MoM matrix is a transfer function of the structure. The consideration of the excitation at each particular waveguide (V_1 and V_s^j) becomes important when obtaining reflection and transmission parts of the GSM associated with each port.

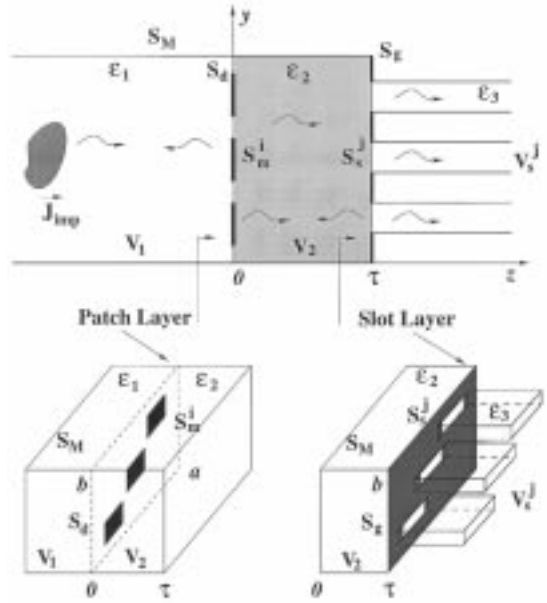

Fig. 2. Geometry of an N-port waveguide-based aperture-coupled patch array transition.

Next we will consider the rectangular waveguide taper for both feeding and collecting. The taper, approximated by double-plane stepped junctions, is modeled using a mode-matching technique in conjunction with the GSM cascading scheme. Finally, each of the waveguide-to-microstrip transitions and the amplifying circuitry are modeled as two-port networks. The GSMs of each module are then cascaded using *Agilent ADS* to simulate the overall system response.

B. Integral Equation Formulation for an N-Port Waveguide-Based Aperture-Coupled Patch Array Transition

Our goal is to develop a GSM for an N-port waveguide transition containing an aperture-coupled patch array. A detailed procedure resulting in the GSM of closely spaced electric- (strip, patch) and magnetic-type (slot, aperture) surfaces in a two-port waveguide was presented in [17]. The same methodology is adopted here for the modeling of the N-port waveguide transition shown in Fig. 2. This new geometry requires certain modifications of the formulation presented in [17]. These modifications mostly affect the field representations in the waveguides V_s^j and the procedure of deriving the GSM, since the Green's function for each of the waveguides coupled to corresponding slots is different and the procedure requires the consideration of port-to-port coupling for all TE and TM modes.

Similar to [17], a coupled set of integral equations is obtained by enforcing the boundary condition on the tangential components of the electric field on the conductive surfaces (patch array) S_m^i at $z=0$ and the continuity condition on the tangential components of the magnetic field on the magnetic surfaces (slot apertures) S_s^j at $z=\tau$. The integral form of the electric-field boundary condition is obtained using the second vector-dyadic Green's theorem with appropriate boundary and continuity conditions

$$\begin{aligned}\hat{z}\times\overline{\mathbf{E}}_1^{\text{inc}}(\vec{r}) &= \jmath\omega\mu_0\hat{z}\times\sum_{i=1}^{N_m}\int_{S_m^i}\overline{\mathbf{J}}_i(\vec{r}')\cdot\overline{\overline{\mathbf{G}}}_{e1}^{(11)}(\vec{r}',\vec{r})\,dS' \\ &\quad -\hat{z}\times\sum_{j=1}^{N_s}\int_{S_s^j}\overline{\mathbf{M}}_j(\vec{r}')\cdot\left[\nabla'\times\overline{\overline{\mathbf{G}}}_{e1}^{(21)}(\vec{r}',\vec{r})\right]dS'.\end{aligned} \tag{1}$$

The electric dyadic Green's functions of the third kind, $\overline{\overline{\mathbf{G}}}_{e1}^{(11)}(\vec{r},\vec{r}')$ and $\overline{\overline{\mathbf{G}}}_{e1}^{(21)}(\vec{r},\vec{r}')$, are obtained as the solution of the boundary-value problem for a semiinfinite partially filled waveguide (regions V_1 and V_2) terminated by a ground plane at $z=\tau$. They satisfy boundary and continuity conditions for the electric field on the surfaces S_M and S_g and on the interface S_d (details are given in [17]).

The continuity condition for the tangential components of the magnetic field at $z=\tau$ results in the magnetic-field integral equation

$$\begin{aligned}\hat{z}\times\overline{\mathbf{H}}_2^{\text{inc}}(\vec{r}) &= -\frac{\epsilon_2}{\epsilon_1}\hat{z}\times\sum_{i=1}^{N_m}\int_{S_m^i}\overline{\mathbf{J}}_i(\vec{r}')\left[\nabla'\times\overline{\overline{\mathbf{G}}}_{e2}^{(12)}(\vec{r}',\vec{r})\right]dS' \\ &\quad -\jmath\omega\epsilon_0\hat{z}\times\sum_{j=1}^{N_s}\int_{S_s^j}\overline{\mathbf{M}}_j(\vec{r}') \\ &\quad \cdot\left[\epsilon_2\overline{\overline{\mathbf{G}}}_{e2}^{(22)}(\vec{r}',\vec{r})+\epsilon_3\overline{\overline{\mathbf{G}}}_{e2}^{(j)}(\vec{r}',\vec{r})\right]dS'.\end{aligned} \tag{2}$$

The electric dyadic Green's functions of the third kind, $\overline{\overline{\mathbf{G}}}_{e2}^{(12)}(\vec{r},\vec{r}')$ and $\overline{\overline{\mathbf{G}}}_{e2}^{(22)}(\vec{r},\vec{r}')$, have been derived for a semiinfinite partially filled waveguide (regions V_1 and V_2) satisfying boundary and continuity conditions for the magnetic field vector (formulation of the boundary-value problem is given in [17]). The electric dyadic Green's functions of the second kind $\overline{\overline{\mathbf{G}}}_{e2}^{(j)}(\vec{r},\vec{r}')$ are obtained for the semiinfinite waveguides (regions V_s^j) terminated by a ground plane at $z=\tau$. The slot-to-waveguide interface at $z=\tau$ is shown in Fig. 3. Note that each slot is associated with the corresponding single-mode waveguide. Green's functions are obtained in terms of double series expansions over the complete system of eigenfunctions of the Helmholtz operator (see the Appendix).

The incident electric $\overline{\mathbf{E}}_1^{\text{inc}}(\vec{r})$ and magnetic $\overline{\mathbf{H}}_2^{\text{inc}}(\vec{r})$ fields are expressed as a series eigenmode expansion for all propagating and evanescent TE and TM modes. The electric and magnetic vector functions in this expansion satisfy the unity power normalization condition [20]. Complete expressions for the incident electric and magnetic field (with the excitation in the region V_1) are given in [17].

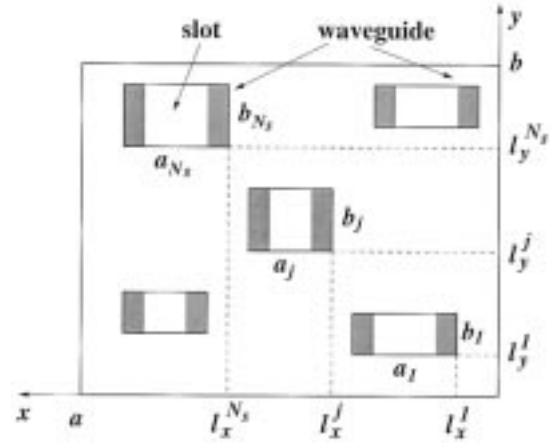

Fig. 3. Cross section of a slot-to-waveguide interface at $z=\tau$.

The MoM discretization for the electric and magnetic currents enables the reduction of a coupled set of functional equations, (1) and (2), to a matrix system of algebraic equations with respect to the unknown coefficients in the currents expansion. The x- and y-directed overlapping piecewise sinusoidal basis and testing functions are used for the electric and magnetic currents expansion. A matrix system of linear equations is obtained in the form similar to [17]

$$\mathbf{A}\,\mathbf{X}=\mathbf{F}^{\text{inc}} \tag{3}$$

where $\mathbf{A}$ is the total MoM matrix of all self- and mutual interactions of electric and magnetic field components with the electric and magnetic current components associated with each waveguide port

$$\mathbf{A}=\begin{bmatrix}\jmath\omega\mu_0\mathbf{Z}(\omega) & \mathbf{U}(\omega)\\ \mathbf{W}(\omega) & -\jmath\omega\epsilon_0\mathbf{Y}(\omega)\end{bmatrix}.$$

$\mathbf{X}$ is the vector of unknown current coefficients and $\mathbf{F}^{\text{inc}}$ represents tested incident electric and magnetic fields

$$\mathbf{X}=\begin{bmatrix}\mathbf{J}\\ \mathbf{M}\end{bmatrix},\qquad \mathbf{F}^{\text{inc}}=\begin{bmatrix}\mathbf{V}\\ \mathbf{I}\end{bmatrix}.$$

Note that $\mathbf{F}^{\text{inc}}$ is obtained in terms of magnitudes of all propagating and evanescent TE and TM modes in the eigenmode expansion for the incident electric and magnetic field. The elements $\mathbf{Z}$, $\mathbf{U}$, $\mathbf{W}$, $\mathbf{Y}$ of the MoM block-matrix $\mathbf{A}$ are associated with the electric or magnetic field due to electric or magnetic current, respectively, generated at each waveguide of the N-port transition. Inverting the MoM matrix $\mathbf{A}$ results in the solution of (3) for the magnitudes of electric and magnetic currents

$$\begin{bmatrix}\mathbf{J}\\ \mathbf{M}\end{bmatrix}=\mathbf{A}^{-1}\begin{bmatrix}\mathbf{V}\\ \mathbf{I}\end{bmatrix}. \tag{4}$$

In this section, we summarized the integral equation formulation for an aperture-coupled patch array in the N-port waveguide transition. The main goal here was to express the magnitudes of the electric and magnetic currents in terms of the inverted MoM matrix and the magnitudes of the incident TE and

TM modes. This result is used for the further development of the GSM of the transition.

C. Scattering Parameters

The GSM of the N-port waveguide transition relates magnitudes of incident and scattered (reflected and transmitted) propagating and evanescent TE and TM modes. The integral form representation and eigenmode expansion for scattered fields enables one to express the magnitudes of scattered modes in terms of electric and magnetic currents induced on the surfaces of patch and slot arrays. This was implemented in [17] for the two-port waveguide transition. In the N-port transition with the incident field in the region V_1, the magnitudes b_{mn} of reflected TE and TM modes at the interface $z = 0$ can be obtained in the following form:

$$\begin{aligned}\begin{Bmatrix} b_{mn}^{-\mathrm{TE}} \\ b_{mn}^{-\mathrm{TM}} \end{Bmatrix} &= -\jmath\omega\mu_0 \sum_{i=1}^{N_m} \int_{S_w} \int_{S_m^i} \left[\overline{\mathbf{J}}_i \cdot \overline{\overline{\mathbf{G}}}_{e1}^{(11)} \begin{Bmatrix} \overline{\mathbf{h}}_{mn}^{-\mathrm{TE}} \\ \overline{\mathbf{h}}_{mn}^{-\mathrm{TM}} \end{Bmatrix} \right] \\ &\quad \cdot (-\hat{z})\, dS'\, dS + \sum_{j=1}^{N_s} \int_{S_w} \int_{S_s^j} \left[\overline{\mathbf{M}}_j \cdot \left[\nabla' \times \overline{\overline{\mathbf{G}}}_{e1}^{(21)} \right] \right. \\ &\quad \left. \times \begin{Bmatrix} \overline{\mathbf{h}}_{mn}^{-\mathrm{TE}} \\ \overline{\mathbf{h}}_{mn}^{-\mathrm{TM}} \end{Bmatrix} \right] \\ &\quad \cdot (-\hat{z}) dS'\, dS + \begin{Bmatrix} a_{mn}^{+\mathrm{TE}} \\ a_{mn}^{+\mathrm{TM}} \end{Bmatrix} \begin{Bmatrix} R_{mn}^{\mathrm{TE}} \\ R_{mn}^{\mathrm{TM}} \end{Bmatrix} \end{aligned} \tag{5}$$

where

- $\pm$ waves propagating in the positive $(+)$ and negative $(-)$ z-directions;
- S_w V_1 waveguide cross section;
- $\overline{\mathbf{h}}_{mn}$ magnetic vector functions;
- R_{mn} total reflection coefficients at $z = 0$ (obtained in [17]);
- a_{mn} magnitudes of incident modes.

The expressions for the electric and magnetic vector function components for TE and TM modes normalized by the unity power have been derived using the procedure described in [20].

The magnitudes c_{mnj} of TE and TM modes transmitted into the waveguides V_s^j with the excitation in the region V_1 are expressed in terms of induced magnetic currents at the interface $z = \tau$

$$\begin{Bmatrix} c_{mnj}^{+\mathrm{TE}} \\ c_{mnj}^{+\mathrm{TM}} \end{Bmatrix} = -\int_{S_w^j} \int_{S_s^j} \left[\overline{\mathbf{M}}_j \cdot \left[\nabla' \times \overline{\overline{\mathbf{G}}}_{e1}^{(j)} \right] \times \begin{Bmatrix} \overline{\mathbf{h}}_{mnj}^{+\mathrm{TE}} \\ \overline{\mathbf{h}}_{mnj}^{+\mathrm{TM}} \end{Bmatrix} \right] \cdot \hat{z}\, dS'\, dS \tag{6}$$

where S_w^j and $\overline{\mathbf{h}}_{mnj}$ are the cross-sectional area and magnetic vector functions, respectively, associated with the waveguides V_s^j. The electric dyadic Green's functions of the first kind, $\overline{\overline{\mathbf{G}}}_{e1}^{(j)}(\vec{r}, \vec{r}')$, are obtained for semiinfinite waveguides V_s^j of dielectric permittivity ϵ_3 terminated by a ground plane at $z = \tau$, which are similar to $\overline{\overline{\mathbf{G}}}_{e2}^{(j)}$ shown in the Appendix except for the boundary conditions of the first kind. Note that the magnitudes of electric and magnetic currents in (4) are obtained in terms of magnitudes of incident TE and TM modes. Substituting (4) into (5) and (6) results in a matrix representation relating the magnitudes a_{mn} of incident modes and the magnitudes b_{mn} and c_{mnj} of reflected and transmitted modes, respectively. This matrix represents the reflected and transmitted parts of the GSM of the N-port transition when the incident field is generated in region V_1.

The next step in this procedure is to obtain the GSM for reflected and transmitted modes with the excitation at each of the waveguides V_s^j. The integral form representation and eigenmode expansion of reflected and incident modes yield the expression for the magnitudes b_{mnj} of reflected and transmitted (coupled to $N_s - 1$ waveguides V_s^j) modes at $z = \tau$

$$\begin{aligned}\begin{Bmatrix} b_{mnj}^{+\mathrm{TE}} \\ b_{mnj}^{+\mathrm{TM}} \end{Bmatrix} &= -\jmath\omega\epsilon_0\epsilon_3 \int_{S_w^j} \int_{S_s^j} \begin{Bmatrix} \overline{\mathbf{e}}_{mnj}^{+\mathrm{TE}} \\ \overline{\mathbf{e}}_{mnj}^{+\mathrm{TM}} \end{Bmatrix} \times \left[\overline{\mathbf{M}}_j \cdot \overline{\overline{\mathbf{G}}}_{e2}^{(j)} \right] \\ &\quad \cdot \hat{z}\, dS'\, dS - \delta_{jk} \begin{Bmatrix} a_{mnk}^{-\mathrm{TE}} \\ a_{mnk}^{-\mathrm{TM}} \end{Bmatrix} \end{aligned} \tag{7}$$

where

- δ_{jk} Kronecker delta;
- $\overline{\mathbf{e}}_{mnj}$ electric vector functions of the waveguides V_s^j;
- a_{mnk} magnitudes of incident modes in the kth waveguide ($k = 1, \ldots, N_s$).

The magnitudes c_{mnk} of TE and TM modes transmitted into the waveguide V_1 (the incident field is generated in the waveguides V_s^j) are obtained at $z = 0$ in terms of induced electric and magnetic currents

$$\begin{aligned}\begin{Bmatrix} c_{mnk}^{-\mathrm{TE}} \\ c_{mnk}^{-\mathrm{TM}} \end{Bmatrix} &= \sum_{i=1}^{N_m} \int_{S_w} \int_{S_m^i} \begin{Bmatrix} \overline{\mathbf{e}}_{mn}^{-\mathrm{TE}} \\ \overline{\mathbf{e}}_{mn}^{-\mathrm{TM}} \end{Bmatrix} \\ &\quad \times \overline{\mathbf{J}}_i \cdot \left[\nabla' \times \overline{\overline{\mathbf{G}}}_{e2}^{(11)} \right] \cdot (-\hat{z})\, dS'\, dS \\ &\quad + \jmath\omega\epsilon_0\epsilon_1 \sum_{j=1}^{N_s} \delta_{jk} \int_{S_w} \int_{S_s^j} \begin{Bmatrix} \overline{\mathbf{e}}_{mn}^{-\mathrm{TE}} \\ \overline{\mathbf{e}}_{mn}^{-\mathrm{TM}} \end{Bmatrix} \\ &\quad \times \left[\overline{\mathbf{M}}_j \cdot \overline{\overline{\mathbf{G}}}_{e2}^{(21)} \right] \cdot (-\hat{z})\, dS'\, dS \end{aligned} \tag{8}$$

where $\overline{\mathbf{e}}_{mn}$ are the electric vector functions of the waveguide V_1. The electric dyadic Green's functions of the third kind, $\overline{\overline{\mathbf{G}}}_{e2}^{(11)}(\vec{r}, \vec{r}')$, $\overline{\overline{\mathbf{G}}}_{e2}^{(21)}(\vec{r}, \vec{r}')$, have been derived for a semiinfinite partially filled waveguide (regions V_1 and V_2 with the point source located in region V_1) satisfying boundary and continuity conditions for the magnetic field vector.

In the case of excitation from the waveguides V_s^j, the MoM procedure results in the following representation for the magnitudes of induced electric and magnetic currents:

$$\begin{bmatrix} \mathbf{J} \\ \mathbf{M} \end{bmatrix} = \mathbf{A}^{-1} \begin{bmatrix} \mathbf{0} \\ \mathbf{I} \end{bmatrix}. \tag{9}$$

The result (9) together with (7) and (8) leads to the GSM representation for reflected and transmitted modes for the case when the incident magnetic field is generated at each of the waveguides V_s^j, one at a time. It should be noted that in this formulation, a coupling of all propagating and evanescent TE and TM modes from all ports is taken into account.

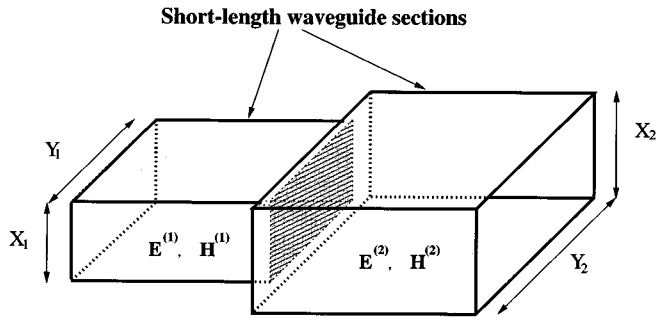

Fig. 4. A double-step junction of two rectangular waveguides.

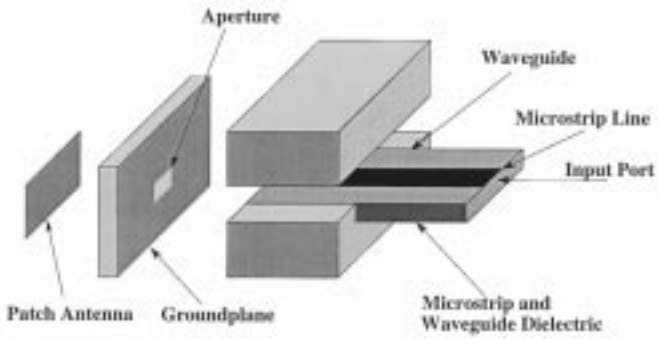

Fig. 5. A waveguide-to-microstrip line junction.

In this section, we described a procedure to construct the GSM of an aperture-coupled patch array in the N-port waveguide transition. This was developed to obtain an overall response of the system by cascading GSMs of the waveguide transitions, rectangular waveguide tapers, waveguide-to-microstrip line junctions, and the S-parameters of amplifier circuits.

D. Rectangular Waveguide Taper

The feeding and collecting waveguide tapers, approximated by double-plane stepped junctions, are analyzed using the mode-matching technique similar to [18]. The mode-matching technique is known to be an efficient method for calculating the GSM of horn antennas and tapered waveguides. The two important parameters in the discretization are the number of steps and the number of waveguide modes, which both depend on the flaring angle of the transition and the frequency of operation. A double-step plane junction is shown in Fig. 4, where X_1 and Y_1 are the smaller waveguide dimensions and X_2 and Y_2 are the larger waveguide dimensions. At the double-step plane discontinuity, the total field can be expressed as a superposition of an infinite number of evanescent and propagating TE and TM modes. The GSM for each junction is then obtained by matching the total power of all modes at both sides of the junction. Finally, the overall GSM of the whole waveguide taper is obtained by cascading the individual GSMs. In order to make the simulation more accurate, higher order modes were included while internally cascading the double-step junctions. However, due to the symmetry of the structure, only even modes are excited. In addition, there is no need to include many higher order modes in the overall cascading procedure, since most of the energy is in the first few modes.

E. Waveguide-to-Microstrip Line Feed Junction

The waveguide-to-microstrip-to-aperture-coupled patch antenna (shown in Fig. 5) was designed using *Agilent HFSS*. This consists of microstrip-to-waveguide and waveguide-to-aperture-coupled patch antenna transitions. The design of the microstrip-to-waveguide transition was performed first by matching the impedance of the waveguide to that of the microstrip line. The entire antenna feed was then simulated to obtain a resonant frequency of 10 GHz and a 10-dB return loss bandwidth of 400 MHz [15]. A more detailed discussion of the design process can be found in [19]. The simulation of the antenna feed has been incorporated in the simulation of the array discussed earlier.

III. Numerical and Experimental Results

The above-mentioned procedure for cascading the individual modules is implemented using a commercial circuit simulator, *Agilent ADS*, where both waveguide modes and physical ports are treated as circuit ports. Even though the measured S-parameters of the amplifiers were incorporated into the circuit simulation, any nonlinear model can be used to characterize the amplifiers. Hence, the initial goal of modeling the interaction between active devices and electromagnetic environment is achieved.

In order to verify the accuracy of the full-wave modeling, two experiments were to be performed on a previously published amplifier array at X-band [15], [19]. The two experiments consist of the measurement of a unit cell and a 2×3 array, as shown in Fig. 1. Each unit cell of the two experiments contained an input aperture-coupled patch antenna, a waveguide-to-microstrip transition, a two-stage amplifying circuit, a second microstrip-to-waveguide transition, and an output aperture-coupled patch antenna. In the single unit cell measurement, a WR90 waveguide was used to feed the input and output antennas. The waveguide was placed in contact with the ground plane, and the dielectric of the patch antenna was fit within the waveguide walls. The patch antennas have 340 mil width and 320 mil height; the slots are of 250 mil width and 15 mil height; and the substrate thickness is 31 mil with permittivity of 2.2. The dielectric-filled waveguide has 450 mil width, 15 mil height, and 100 mil length. The total length of the microstrip circuit including two amplifiers is 1800 mil, and the width of the microstrip line is 45 mil. The numerical model of the dielectric-filled waveguide-to-patch antenna-to-WR90 waveguide was combined with measured data of the amplifier circuit and simulated microstrip-to-waveguide transitions. The results for the complete numerical model and experiment are shown in Fig. 6. The numerical model for the single unit cell predicted the behavior of the circuit well and compares better with measured results than a commercial 3-D FEM program. It should be noted that the FEM commercial programs are not capable of modeling the overmoded spatial power combining array presented in this paper due to the excessive memory requirements.

The second experiment was performed in the same manner as the first experiment. For the 2×3 array, a horn 1200 mil high, 1811 mil wide, and 1633 mil long was used to feed the array at both the input and output. Unit cells in the array are separated by a distance of 600 mil. The array was placed within the center

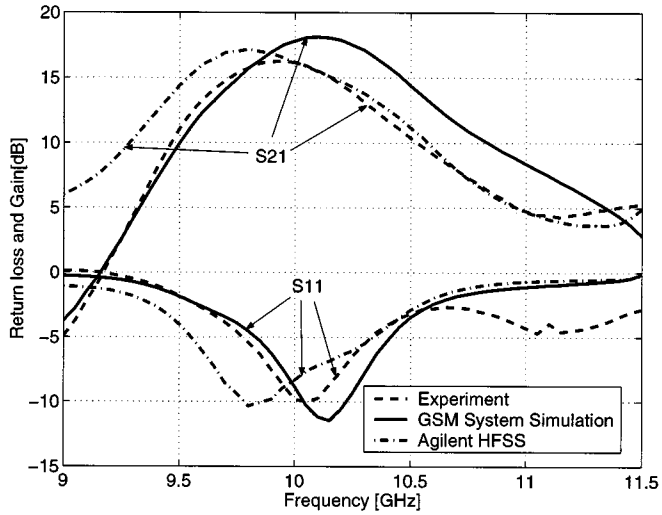

Fig. 6. Numerical and experimental results for the return loss and gain of the single aperture-coupled patch amplifier waveguide transition.

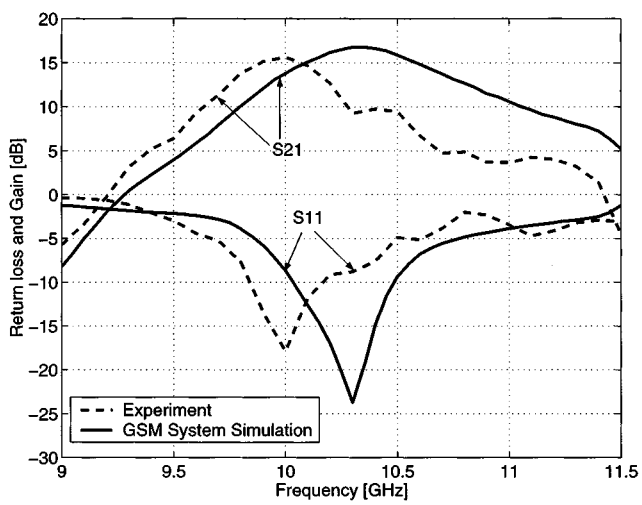

Fig. 7. Numerical and experimental results for the return loss and gain of the 2×3 waveguide-based aperture-coupled patch amplifier array.

of the horn so that the ground plane of the array was in contact with the aperture of the horn. The numerical and experimental results for the return loss and gain for the 2×3 array are shown in Fig. 7. The numerical model of the array favorably predicts the change in the resonant frequency and gain caused by the cascading of the horn and waveguide-to-antenna GSMs. This behavior is not apparent when only considering the dominant mode coupling from the waveguide-to-aperture-coupled patch array.

The authors believe that some disagreement between theory and experiment was due to lack of precision in the experimental setup. In the experiment, the excitation waveguide or hard-horn antenna does not provide a continuous contact between itself and the array, as was assumed in the simulation. Also, the simulation does not include conductor and dielectric losses. In addition, the interface between the slot ground plane and that of the dielectric filled waveguides was not continuous.

IV. Conclusion

Electromagnetic modeling and experimental verification were presented for the accurate analysis of a complete waveguide-based spatial power-combining array. This is accomplished by decomposing the system into electromagnetically coupled modules, including rectangular waveguide tapers, aperture-coupled patch array-to-waveguide transitions, waveguide-to-microstrip line junctions, and amplifier networks. The overall response of the system was obtained by cascading GSMs of passive elements and the S-parameters of the amplifier networks. Numerical and experimental results were shown for a single unit cell and 2×3 amplifier arrays. This methodology can be effectively used for the electromagnetic modeling of various waveguide-based spatial and quasi-optical power-combining systems containing planar transverse patch and slot amplifier arrays, leading to a better understanding of multimoding and surface-wave coupling effects and field-circuit interaction mechanisms.

Appendix
Electric Dyadic Green's Functions of the Second Kind

The electric dyadic Green's functions of the second kind, $\overline{\overline{\mathbf{G}}}_{e2}^{(j)}(\vec{r}, \vec{r}')$, are obtained for semiinfinite rectangular waveguides of dielectric permittivity ϵ_3 and terminated by a ground plane at $z = \tau$. The cross section of waveguide-to-slot interface is shown in Fig. 3. The functions determined as the solution of dyadic differential equations with a point source positioned in the waveguides V_s^j

$$\nabla \times \nabla \times \overline{\overline{\mathbf{G}}}_{e2}^{(j)}(\overline{r}, \overline{r}') - k_3^2 \overline{\overline{\mathbf{G}}}_{e2}^{(j)}(\overline{r}, \overline{r}') = \overline{\overline{\mathbf{I}}}\delta(\overline{r} - \overline{r}'), \quad \overline{r}, \overline{r}' \in V_s^j,\ j = 1, \ldots, N_s \tag{10}$$

subject to boundary conditions of the second kind on the waveguide surface S_M, surface of the ground plane S_g, and surfaces of slots S_s^j

$$\hat{n} \times \nabla \times \overline{\overline{\mathbf{G}}}_{e2}^{(j)}(\overline{r}, \overline{r}') = 0, \qquad \hat{n} \cdot \overline{\overline{\mathbf{G}}}_{e2}^{(j)}(\overline{r}, \overline{r}') = 0, \qquad \overline{r} \in S_M \cup S_g \cup S_s^j \tag{11}$$

and the radiation condition at infinity.

Components of the Green's dyadic are expressed in terms of a double series expansion over the complete system of eigenfunctions of the Helmholtz operator

$$G_{e2,pr}^{(j)} = \sum_{m=0}^{\infty} \sum_{n=0}^{\infty} \psi_{mn}^{p(j)}(x, y) \psi_{mn}^{r(j)}(x', y') f_{mn,pr}^{(j)} \qquad p, r = x, y \tag{12}$$

where $\psi_{mn}^{p(j)}(x, y)$ are orthonormal eigenfunctions of the two-dimensional Helmholtz operator subject to the second kind boundary conditions on the metal surface of waveguide cross section

$$\psi_{mn}^{x(j)}(x, y) = \sqrt{\frac{\epsilon_{0m}\epsilon_{0n}}{a_j b_j}} \sin(k_{xj}(x - l_x^j)) \cos(k_{yj}(y - l_y^j))$$

$$\psi_{mn}^{y(j)}(x, y) = \sqrt{\frac{\epsilon_{0m}\epsilon_{0n}}{a_j b_j}} \cos(k_{xj}(x - l_x^j)) \sin(k_{yj}(y - l_y^j))$$

$$\psi_{mn}^{z(j)}(x, y) = \sqrt{\frac{\epsilon_{0m}\epsilon_{0n}}{a_j b_j}} \cos(k_{xj}(x - l_x^j)) \cos(k_{yj}(y - l_y^j)). \tag{13}$$

Here

$$k_{xj} = \frac{m\pi}{a_j}, \quad k_{yj} = \frac{n\pi}{b_j}$$

and ϵ_{0m}, ϵ_{0n} are Newman indexes such that $\epsilon_{00} = 1$, and $\epsilon_{0m} = 2$, $m \neq 0$.

The characteristic Green's functions $f^{(j)}_{mn,pr}(z, z')$ are obtained as the solution of a one-dimensional scalar wave equation forced with a $\delta(z - z')$ function and satisfying boundary conditions (11) reduced to the one-dimensional ones using orthonormal properties of eigenfunctions

$$f^{(j)}_{mn,xx} = \frac{(k_3^2 - k_{xj}^2)}{2\gamma_j k_3^2}\left[e^{-\gamma_j|z-z'|} + e^{-\gamma_j(z+z'-2\tau)}\right]$$

$$f^{(j)}_{mn,xy} = f^{(j)}_{mn,yx} = -\frac{k_{xj}k_{yj}}{2\gamma_j k_3^2}\left[e^{-\gamma_j|z-z'|} + e^{-\gamma_j(z+z'-2\tau)}\right]$$

$$f^{(j)}_{mn,yy} = \frac{(k_3^2 - k_{yj}^2)}{2\gamma_j k_3^2}\left[e^{-\gamma_j|z-z'|} + e^{-\gamma_j(z+z'-2\tau)}\right] \tag{14}$$

where γ_j is the propagation constant defined as

$$\gamma_j = \begin{cases} \jmath\sqrt{k_3^2 - k_{xj}^2 - k_{yj}^2}, & k_3^2 > k_{xj}^2 + k_{yj}^2 \\ \sqrt{k_{xj}^2 + k_{yj}^2 - k_3^2}, & k_3^2 < k_{xj}^2 + k_{yj}^2. \end{cases}$$

Note that the transverse components of the Green's functions $\overline{\overline{\mathbf{G}}}^{(j)}_{e2}$ are primarily of interest, as they appear in the integral equation formulation for planar transverse magnetic-type surfaces.

REFERENCES

[1] M. Kim, J. J. Rosenberg, R. P. Smith, R. M. Weikle, J. B. Hacker, M. P. Delisio, and D. B. Rutledge, "A grid amplifier," *IEEE Microwave Guided Wave Lett.*, vol. 1, pp. 322–324, Nov. 1991.

[2] M. Kim, E. A. Sovero, J. B. Hacker, M. P. Delisio, J.-C. Chiao, S.-J. Li, D. R. Gagnon, J. J. Rosenberg, and D. B. Rutledge, "A 100-element HBT grid amplifier," *IEEE Trans. Microwave Theory Tech.*, vol. 41, pp. 1762–1771, Oct. 1993.

[3] C.-Y. Chi and G. M. Rebeiz, "A quasioptical amplifier," *IEEE Microwave Guided Wave Lett.*, vol. 3, pp. 164–166, June 1993.

[4] T. Ivanov, A. Balasubramaniyan, and A. Mortazawi, "One- and two-stage spatial amplifiers," *IEEE Trans. Microwave Theory Tech.*, vol. 43, pp. 2138–2143, Sept. 1995.

[5] M. N. Abdulla, U. A. Mughal, H.-S. Tsai, M. B. Steer, and R. A. York, "A full-wave system simulation of a folded-slot spatial power combining amplifier array," in *IEEE MTT-S Int. Microwave Symp. Dig.*, June 1999, pp. 559–562.

[6] T. Ivanov and A. Mortazawi, "A two-stage spatial amplifier with hard horn feeds," *IEEE Microwave Guided Wave Lett.*, vol. 6, pp. 88–90, Feb. 1996.

[7] M. A. Ali, S. C. Ortiz, T. Ivanov, and A. Mortazawi, "Analysis and measurement of hard-horn feeds for the excitation of quasioptical amplifiers," *IEEE Trans. Microwave Theory Tech.*, vol. 47, pp. 479–487, Apr. 1999.

[8] J. Sowers, D. Pritchard, A. White, W. Kong, and O. Tang, "A 36 W, V-band, solid state source," *IEEE MTT-S Int. Microwave Symp. Dig.*, pp. 235–238, June 1999.

[9] J. Hubert, L. Mirth, S. Ortiz, and A. Mortazawi, "A 4 watt Ka-band quasioptical amplifier," in *IEEE MTT-S Int. Microwave Symp. Dig.*, June 1999, pp. 551–554.

[10] A. Alexanian and R. A. York, "Broadband waveguide-based spatial combiners," in *IEEE MTT-S Int. Microwave Symp. Dig.*, June 1997, pp. 1139–1142.

[11] N.-S. Cheng, A. Alexanian, M. G. Case, and R. A. York, "20 watt spatial power combiner in waveguide," in *IEEE MTT-S Int. Microwave Symp. Dig.*, June 1998, pp. 1457–1460.

[12] N.-S. Cheng, A. Alexanian, M. G. Case, D. B. Rensch, and R. A. York, "40-W CW broad-band spatial power combiner using dense finline arrays," *IEEE Trans. Microwave Theory Tech.*, vol. 47, pp. 1070–1076, July 1999.

[13] N.-S. Cheng, T.-P. Dao, M. G. Case, D. B. Rensch, and R. A. York, "A 60-watt X-band spatially combined solid-state amplifier," in *IEEE MTT-S Int. Microwave Symp. Dig.*, June 1999, pp. 539–542.

[14] N.-S. Cheng, P. Jia, D. B. Rensch, and R. A. York, "A 120-W X-band spatially combined solid-state amplifier," *IEEE Trans. Microwave Theory Tech.*, vol. 47, pp. 2557–2561, Dec. 1999.

[15] S. Ortiz and A. Mortazawi, "A perpendicularly-fed patch array for quasioptical power combining," in *IEEE MTT-S Int. Microwave Symp. Dig.*, June 1999, pp. 667–670.

[16] A. B. Yakovlev, A. I. Khalil, C. W. Hicks, and M. B. Steer, "Electromagnetic modeling of a waveguide-based strip-to-slot transition module for application to spatial power combining systems," in *Proc. IEEE AP-S Int. Symp.*, July 1999, pp. 286–289.

[17] A. B. Yakovlev, A. I. Khalil, C. W. Hicks, A. Mortazawi, and M. B. Steer, "The generalized scattering matrix of closely spaced strip and slot layers in waveguide," *IEEE Trans. Microwave Theory Tech.*, vol. 48, pp. 126–137, Jan. 2000.

[18] H. Patzelt and F. Arndt, "Double-plane steps in rectangular waveguides and their application for transformers, irises, and filters," *IEEE Trans. Microwave Theory Tech.*, vol. 30, pp. 771–776, May 1982.

[19] S. Ortiz and A. Mortazawi, "A perpendicular aperture-fed patch antenna for quasioptical amplifier arrays," in *IEEE AP-S Int. Symp.*, July 1999, pp. 2386–2389.

[20] R. E. Collin, *Field Theory of Guided Waves*. New York: IEEE Press, 1991.

Alexander B. Yakovlev (S'94–M'97) was born in Ukraine on June 5, 1964. He received the Ph.D. degree in radiophysics from the Institute of Radiophysics and Electronics, National Academy of Sciences, Ukraine, in 1992 and the Ph.D. degree in electrical engineering from the University of Wisconsin at Milwaukee in 1997.

From 1992 to 1994, he was an Assistant Professor in the Department of Radiophysics, Dniepropetrovsk State University, Ukraine. From 1994 to 1997, he was a Research and Teaching Assistant in the Department of Electrical Engineering and Computer Science, University of Wisconsin at Milwaukee. From 1997 to 1998, he was an R&D Engineer in the Compact Software Division, Ansoft Corporation, Pittsburgh, PA. From 1998 to 2000, he was a Postdoctoral Research Associate in the Electrical and Computer Engineering Department, North Carolina State University, Raleigh. In summer 2000, he joined the Department of Electrical Engineering, The University of Mississippi, University, as an Assistant Professor. His research interests include mathematical methods in applied electromagnetics, modeling of high-frequency interconnection structures and amplifier arrays for spatial and quasi-optical power combining, integrated-circuit elements and devices, theory of leaky waves, and singularity theory.

Dr. Yakovlev received the Young Scientist Award presented at the 1992 URSI International Symposium on Electromagnetic Theory, Sydney, Australia, and the Young Scientist Award at the 1996 International Symposium on Antennas and Propagation, Chiba, Japan.

Sean Ortiz (S'96) received the B.S.E.E. and M.S.E.E. degrees from the University of Central Florida, Orlando, in 1996 and 1998, respectively. He is currently pursuing the Ph.D. degree in electrical engineering at North Carolina State University, Raleigh.

His research interests include quasi-optical power-combining amplifiers, electromagnetically hardened horns, and transmit-receive antennas.

Mr. Ortiz is a National Science Foundation Graduate Fellow and a member of Tau Beta Pi.

Mete Ozkar (S'97) received the B.S. degree in electrical engineering from the Middle East Technical University, Ankara, Turkey, in 1996 and the M.S. degree from North Carolina State University, Raleigh, in 1998, where he is currently pursuing the Ph.D. degree in electrical engineering.

He is a Research Assistant in the Electronics Research Laboratory, Department of Electrical and Computer Engineering, North Carolina State University, where he performs research in the simulation and the development of spatial power combining systems.

Amir Mortazawi (S'87–M'90) received the B.S. degree from the State University of New York at Stony Brook in 1987 and the M.S. and Ph.D. degrees from the University of Texas, Austin, in 1988 and 1990, respectively, all in electrical engineering.

In 1990, he joined the University of Central Florida, Orlando, as an Assistant Professor, and was promoted to Associate Professor in 1995. In August 1998, he joined North Carolina State University, Raleigh, as an Associate Professor of electrical engineering. His research interests include RF and microwave active circuits, millimiter-wave power-combining oscillators and amplifiers, quasi-optical techniques, and nonlinear analysis of microwave circuits.

Dr. Mortazawi is an Associate Editor for the IEEE TRANSACTIONS ON ANTENNAS AND PROPAGATION.

Michael B. Steer (S'76–M'78–SM'90–F'99) received the B.E. and Ph.D. degrees in electrical engineering from the University of Queensland, Brisbane, Australia, in 1978 and 1983, respectively.

He is currently a Professor of electrical and computer engineering at North Carolina State University, Raleigh, NC. In 1999 and 2000, he was Professor in the School of Electronic and Electrical Engineering, The University of Leeds, where he still holds the Chair in Microwave and Millimeterwave Electronics. He was also Director of the Institute of Microwaves and Photonics, The University of Leeds. His research work has been closely tied to solving fundamental problems in modeling and implementing RF and microwave circuits and systems. His teaching and research interests are in global modeling of the physical layer of RF, microwave, and millimeter-wave electronic systems. His specific research is also directed at RF and microwave design, linearization of efficient power amplifiers, spatial power-combining systems, design of millimeter-wave and terahertz frequency communication and imaging systems, and high-efficiency low-cost RF technologies for wireless applications. He has organized many workshops and has taught many short courses on signal integrity, wireless, and RF design. He has authored or co-authored over 175 refereed papers and book chapters, including approximately 60 journal papers on topics related to RF, microwave, and high-speed digital design methodology. He has co-authored one book and holds one patent

Prof. Steer is active in the IEEE Microwave Theory and Techniques Society (IEEE MTT-S). In 1997, he was secretary of the Society and was an elected member of the Administrative Committee (AdCom) from 1998 to 2000.